EXTENDING THE INDUCTION PERIOD OF CRYSTALLIZATION FOULING THROUGH SURFACE COATING

T. Geddert[1], I. Bialuch[2], W. Augustin[3] and S.Scholl[4]

[1, 3, 4] Institute for Chemical and Thermal Process Engineering, Langer Kamp 7, 38106 Braunschweig (Germany);
t.geddert@tu-bs.de, w.augustin@tu-bs.de, s.scholl@tu-bs.de
[2] Fraunhofer Institute for Surface Engineering and Thin Films, Bienroder Weg 54E, 38108 Braunschweig (Germany)
ingmar.bialuch@ist.fraunhofer.de

ABSTRACT

To minimize the negative effects of scale formation in heat exchangers, new anti-fouling strategies are focusing on the modification of heat transfer surfaces. These modifications should lead to tailored made surfaces for different technical applications. Aim of this surface modification is the extension of the induction period to minimize the negative effects of fouling and maximize the endurance of the heat exchanger. To achieve such, different surface coatings on stainless steel were investigated in respect of fouling tendency. The effect of flow velocity respectively Reynolds number on the induction time of $CaSO_4$ crystallization fouling were tested in different test units. Diamond like carbon coatings are extending the induction time in every measured flow velocity. At higher Reynolds numbers, the effect of different surface crystallization due to energetic modification is reduced because of the dominating effect of the low adhesive surface. Thus the induction time can be extended by the factor of 2 for low fluid velocities (DLC or SICON®) and more than 20 for higher Reynolds numbers (DLC and SICON®). The combination of limited nucleation spots due to electro-chemical treatment of the substrate before coating can be a tailored made surface with maximum induction time for crystallization fouling.

INTRODUCTION

Fouling of heat exchanger is often induced by the crystallization of inversely soluble salt on the heat transfer surface. Due to this crystallization fouling, an additive layer is formed which leads to an drastic decrease of heat transfer and an increase of pressure drop. The forming of this layer is a function of the process conditions as well as conditions at the heat transfer interface. The influencing factors on crystallization fouling can be subdivided into

- **Process conditions:**
    Salt system, Super-saturation and pH value
    Flow velocity and regime
    Additives
- **Interface conditions:**
    Temperature
    Surface energy, Roughness and Topography
    Amount of nucleation spots
    Aging of the fouling layer and the surface

All these parameter have an influence on the induction time as well as on the crystal growth period (see Fig. 1). A lot of fouling problems in the industry are in defined process
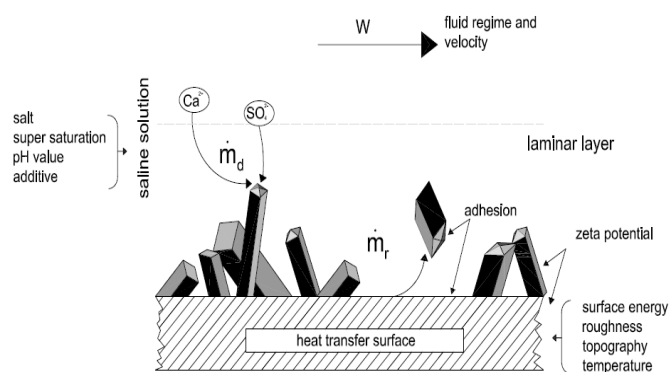

Fig. 1: Deposition and removal in crystallization fouling on heat transfer surfaces

conditions. This reduces the number of influencing variables to the interface conditions. Very common is the energetic modification of the heat transfer surface by different coating techniques [5, 7]. To estimate the potential of coated heat exchanger surfaces, the influence of the energetic modification must be known as well as the possibility to extend the induction time related to the costs of coating. Only if the effect of the modification leads to an drastic lengthening of the induction time equivalent to productivity and decrease of cleaning costs, energetic modification of heat transfer surfaces can find the way to industrial applications.

In crystallization fouling the modification of the interface leads to a change of the relation of removal and growth of crystals on the surface (Eq. 1and Fig. 1) as well as on the growth behavior of the crystals.

$$\frac{dm_f}{dt} = \dot{m}_{deposit} - \dot{m}_{removal} \qquad (1)$$

The coating of the surface should be specially tailored to increase the mass rate of removal or decrease the mass rate of deposit by inhibiting the nucleation. This nucleation takes place in the so called induction period. In this span of time, the heterogeneous nucleation on the heat exchanger surface starts without negative effect on the heat transfer.

Through the crystals formed on the surface the heat transfer can be improved due to turbulence. After the induction period the fouling period occurs were the crystals are forming an compact fouling layer (Fig. 2). This additional crystal layer is reducing heat transfer displayed by the fouling resistance.
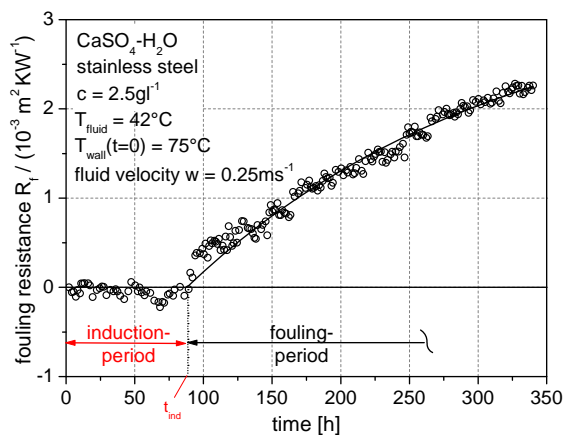

Fig. 2:   Fouling curve of $CaSO_4$ [4]

$$R_f = \frac{1}{k_f} - \frac{1}{k_0} \qquad (2)$$

In this work different coatings are investigated on there fouling tendency in a supersaturated calcium sulfate ($CaSO_4$) solution. The influencing factors surface energy as well as topography have been changed. The coating are made by plasma enhanced chemical vapor deposition (PECVD) and plasma vapor deposition (PVD) technique. The extension of the induction period was investigated with different flow velocities.

EXPERIMENTS

Surface modification

To modify the energetic properties of the heat transfer surface, stainless steel was coated by PECVD. The coating process takes place in an high-vacuum chamber (see Fig 3). The thickness of the coating is 3 μm, therefore the influence of this additional layer compared to the uncoated surface on the heat transfer is negligible. The chamber was evacuated to a base pressure of $< 10^{-3}$ Pa. Before starting the DLC deposition the substrates were cleaned by a sputtering process with Argon ions for a few minutes. To achieve a good adhesion first a silicon containing DLC (a-C:H:Si) interlayer (some 100 nm thick) using tetramethylsilane (TMS: $Si(CH_3)_4$) as a precursor gas were prepared. In the next step the gas composition was changed to a pure

hydrocarbon gas, either methane (CH_4) or acetylene (C_2H_2) for pure DLC films and in some cases TMS or hexamethyldisiloxane (HMDSO) additionally. The PECVD process combined with the thin coating layer ensure a surface near coating were roughness as well as topography are not changed.
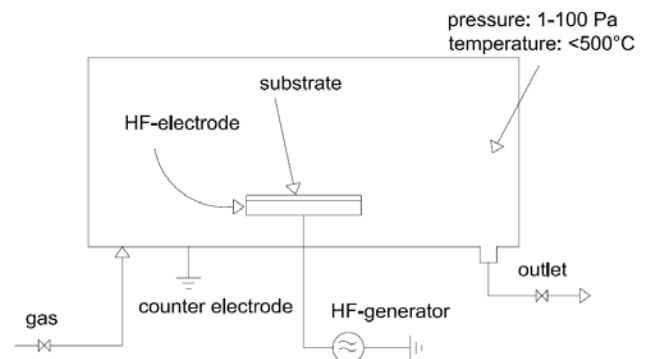

Fig. 3:   Scheme of a PECVD coating unit (modified, from Bewilogua [1])

Within the PECVD process amorphous carbon hydrogen layer were precipitated on the stainless steel surface. Amorphous carbon hydrogen (a-C:H) also called diamond like carbon (DLC) is a very common coating to enhance wear resistance and hardness. In the triangle of diamond, graphite and polymer (see Fig. 4), the surface characteristics of a-C:H coatings can have different rates of polymer, diamond or graphite interactions (detailed description in Trojan [6]).
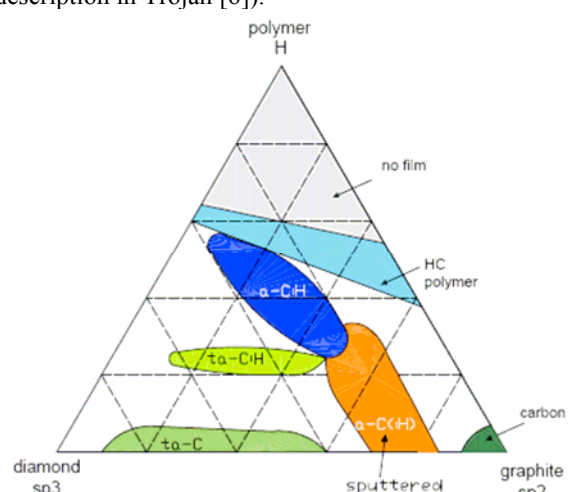

Fig. 4:   Different types of carbon based coatings

The energetic modification of the coating and so the surface energy or contact angle can be changed through defined built-in of different molecules inside the a-C:H matrix. Fig. 5 is showing the water contact angle as a

function of different molecules and concentration inside the a-C:H layer. The increase of silicon inside the coating can change the surface energy from 40 mN/m (DLC) to 36 mN/m (Si-DLC with 15 at.% Si) and finally to 34mN/m (SICAN® with 33 at.% Si). The combination of silicon and oxygen inside the coating can decrease the surface energy to 21 mN/m (SICON®).
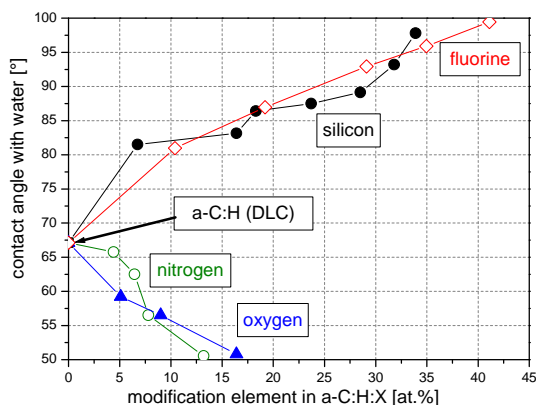

Fig. 5: Influences of different modification elements on the water contact angle for DLC based coatings

Chromium nitrate (CrN) was prepared by a reactive magnetron sputtering process (PVD). The chromium material was emitted from a solid target during a sputtering process in a nitrogen atmosphere. In this case CrN was the coating with the highest surface energy.

Surface characterization

In order to characterize the heat transfer surface before scaling, macroscopic roughness as well as surface topography were investigated. Besides these mechanical surface properties, energetic properties like surface energy are measured to evaluate the achievement of the coating process and investigate the interrelation between surface energy, roughness and fouling tendency. Förster [4, 5] and Zettler [7] negate a direct correlation between surface energy and fouling tendency respectively induction time while most of the authors associate an decrease of roughness with an increase of the induction time.

Surface roughness was investigated with an macroscopic tactile stylus unit (see Fig. 6). For the evaluation of surface contour the R-profile (roughness profile) is deployed which results by filtering the original P-profile (primary profile).
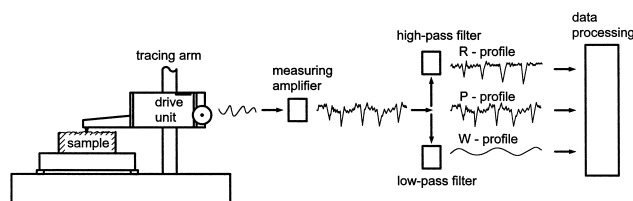

Fig. 6: Macroscopic roughness measurement unit

The data processing unit calculates an integral macroscopic roughness value so called mean roughness depth R_z.

$$R_Z = \frac{1}{5}\sum_{i=1}^{5} Z_i \qquad (3)$$

The increase of the heat transfer surface due to roughness effects is characterised by an atomic force microscope (AFM). The measurement technique is described in detail by Bhushan [2]. The enhancement of the surface is characterized by the interfacial area ratio S_{dr} which is an comparison between real surface and totally flat surface.
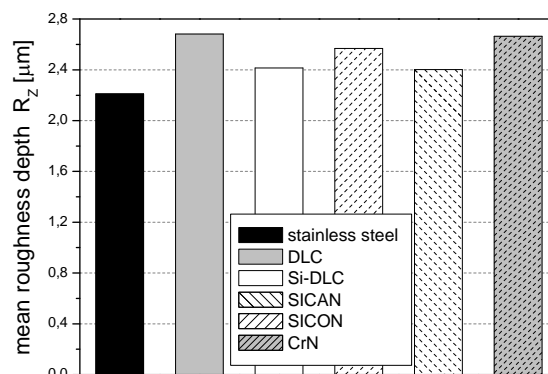

Fig. 7: Mean roughness depth of coated stainless steel

Fig. 7 shows the mean roughness depth of the tested coatings. Through the near surface coating by PECVD, the mean roughness depth is nearly constant, so the effect of roughness on the induction period is negligible.

The macroscopic roughness combined with the enhancement of the heat transfer area is a measure for possible nucleation spots on the surface. Through electrochemical modification of the surface (electropolishing), the amount of nucleation spots can be limited. After the electrochemical treatment of the surface, the heat transfer surfaces can be coated by PECVD. The topography is not effected by the combination of decreasing

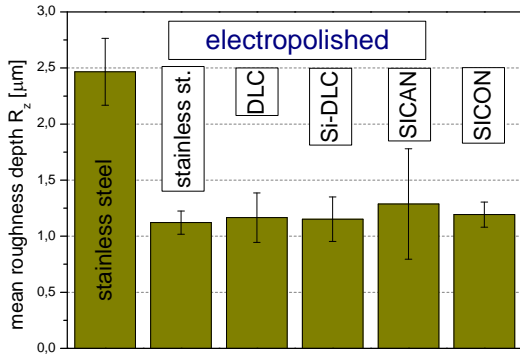the roughness and changing the adhesion properties (see Fig 8).

Fig. 8: Mean roughness depth of coated electropolished stainless steel

To characterize the different energetic modification through PECVD coatings, surface energy was measured with the sessile drop technique. The surface energy should replace the adhesion which should be minimal for optimized process conditions [3]. The principle is based on the measurement of the shape of droplets of different defined liquids. A more detailed description of the surface energy measurement can be found in Förster [4]. Resolving the interfacial free energy, given in Fig. 9, in horizontal direction leads to the Young equation:

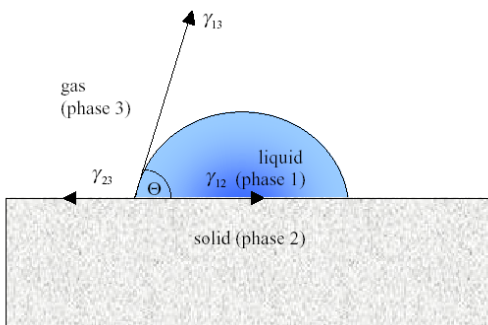$$\gamma_{23} = \gamma_{12} + \gamma_{13} \cdot \cos(\theta) \qquad (4)$$

Fig. 9: Wetting equilibrium

To solve this equation, the missing parameter γ_{12} is replaced by Eq. 5 in the theory of Owens, Wendt, Rabel and Kaelble

$$\gamma_{12} = \gamma_{13}^{LW} + \gamma_{23}^{LW} - 2\left(\sqrt{\gamma_{13}^{dis} \, \gamma_{23}^{dis}} + \sqrt{\gamma_{13}^{pol} \, \gamma_{23}^{pol}} \right) \qquad (5)$$

and reconverted to a linear equation:

$$\frac{\left(1 + \cos(\theta)\right) \cdot \gamma_{13}}{2\sqrt{\gamma_{13}^{D}}} = \sqrt{\gamma_{23}^{P}} \cdot \sqrt{\frac{\gamma_{13}^{P}}{\gamma_{13}^{D}}} + \sqrt{\gamma_{23}^{D}} \qquad (6)$$

The linear fit results out of six point representing the test liquids used for the surface energy calculation:

- o 1-Bromnaphtalene
- o Ethylene glycol
- o Formamide
- o Gylcerin
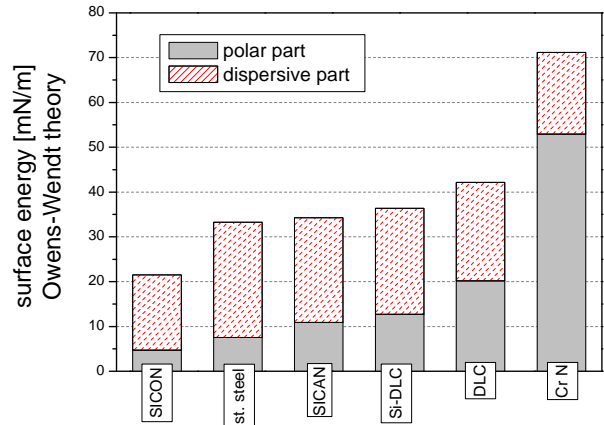- o Methylene iodide
- o Water

Fig. 10: Surface energy of the different coatings on untreated stainless steel

Fig. 10 shows the influence of the 3 μm coated layer on the free surface energy. Related to the untreated stainless steel surface the coating with a-C:H tends to advance the polar part of the surface energy. By defined doping of silicon inside the DLC matrix, the surface energy can be reduced. A combination of oxygen and silicon inside the coating leads to a drastic decrease of the surface energy (SICON®).

Former studies of crystallization fouling [4] show an influence of the macroscopic roughness on the induction time. By an defined decline of the roughness, respectively possible nucleation spots, the induction time may be extended. The combination of mechanic and energetic modification of the surface should reduce the amount of crystallization spots as well as the crystal growth. Fig. 11 shows the influence of the electropolishing of the substrate on the surface energy of the different coatings.
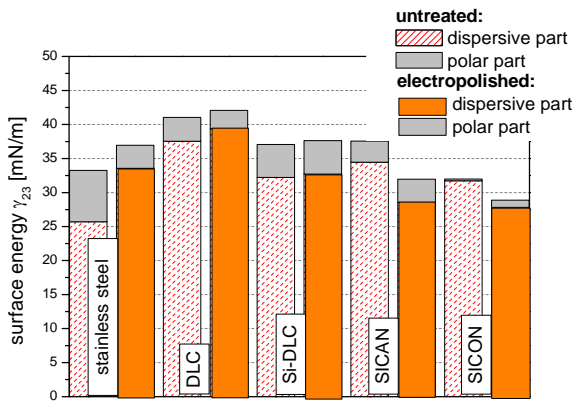
Fig. 11: Surface energy of the different coatings on electro polished stainless steel

Fouling experiments (batch)

Fouling experiments were carried out in a temperature controlled 2.8 l stirred vessel, illustrated in Fig. 12. A slowly rotating stirrer equalizes temperature and concentration gradients. A supersaturated aqueous solution of calcium sulfate with a concentration of 25 mmol/l and a temperature of 42 °C was produced by adding the well dissolvable salts sodium sulfate and calcium chloride. The concentration was quantified by titration and is equal to a saturation index of 0,14.
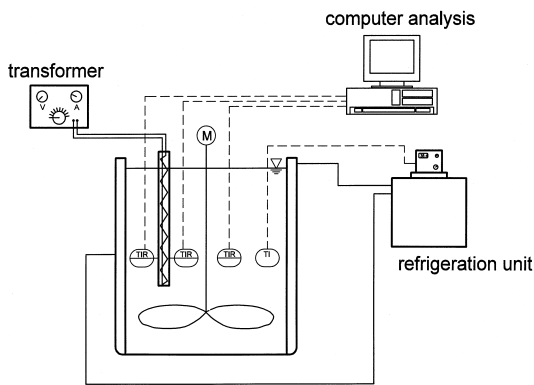

Fig. 12   Batch test unit for fouling experiments

A heating element which consists of a electrical rod heater was immersed in the salt solution. Two thermocouples with a diameter of 1 mm are fixed in grooves on two sides of the heating element. The actual heated plates with the different surfaces can be clamped with brackets on the two sides with the thermocouples. This allows a simple design (80 mm × 20 mm × 2 mm) and an easy assembly of the test items. The surface temperature is adjusted to approximately 75 °C. Measuring quantities are solution temperature, surface temperature of the heating elements and heat duty. Knowing the change of temperature difference between bulk and surface over time allows the calculation of the fouling resistance.
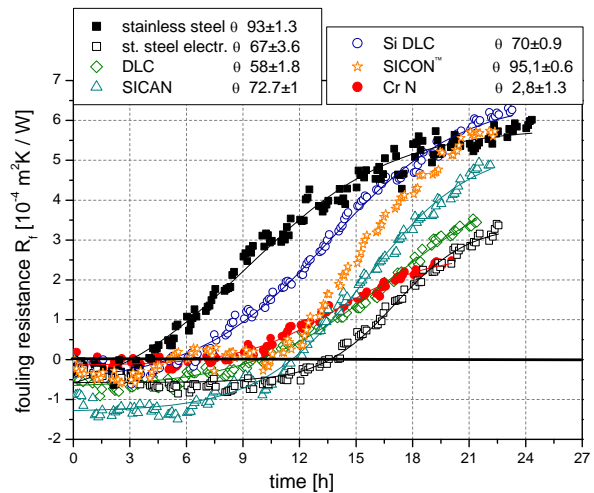

Fig. 13: Fouling curves for different surface materials

Fig. 13 displays the fouling curves for all tested surfaces. After a short induction time the fouling period takes place. The different energetic modifications through surface coating result in different induction time and an extension of the induction period related to the uncoated stainless steel.
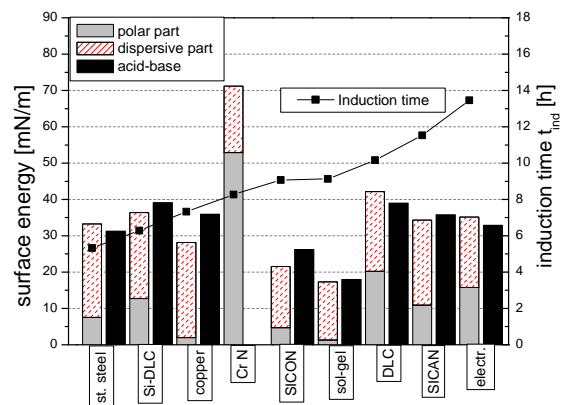

Fig. 14: Surface energy and induction time

Fouling tendency represented by the length of the induction time and surface energy are compared in Fig. 14. The different surface materials are listed with ascending

tendency of the induction time from left to right. The comparison of total surface energy data with induction time yields no correlation between surface energy and fouling behavior. Also the consideration of the polar and disperse parts shows no clear tendency. Thus besides the surface energy and roughness, other interface parameter must have influence on the crystallization fouling. To optimize the anti fouling behavior of coated surfaces, the inhibitory effect of electropolishing on crystallization fouling was combined with the DLC coating.

Fig. 15 displays the effect of electrochemical pretreatment of the substrate before coating on the crystallization fouling. The induction time is comparable to the results of the untreated coated surfaces with no enhancement through the additional process step.
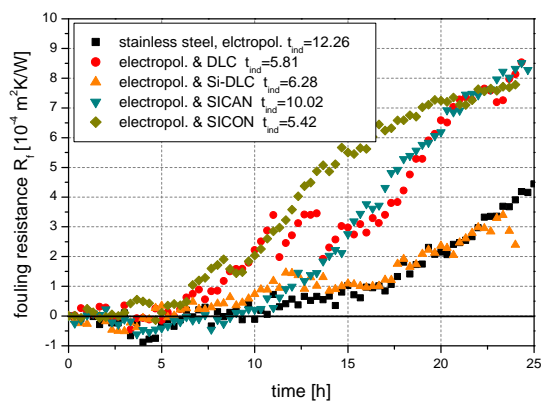

Fig. 15: Fouling curves for different coatings on electro polished stainless steel

Fouling experiments (miniplant)

With constant fluid conditions the fouling process is mainly driven by interface conditions. The fouling process starts with the crystallization on the heat transfer surface following the crystal growth of the formed clusters. The crystallization on different surfaces is a function of the surface conditions (energetic) and the amount of possible nucleation spot (specific roughness). The fouling in real process conditions is mainly driven by the flow conditions. With higher fluid velocity, the mass transport to the surface increases while the interaction between surface and crystal related to the adhesion gets more and more important.

Fouling experiments with defined flow conditions were carried out in a miniplant unit, illustrated in Fig. 16. All process conditions kept constant in comparison to the batch fouling experiments. The 25 mmol/l calcium sulfate solution is preheated to 42 °C and pumped through a valve controlled by a flowmeter in the channel. Inside the channel with a geometry of 18 mm x 15 mm, the coated heat exchanger surfaces (80 mm × 20 mm × 2 mm) are fixed and

heated by a electrical heat rod underneath the flow channel. Two thermocouples under the heated surface allows the calculation of the fouling resistance
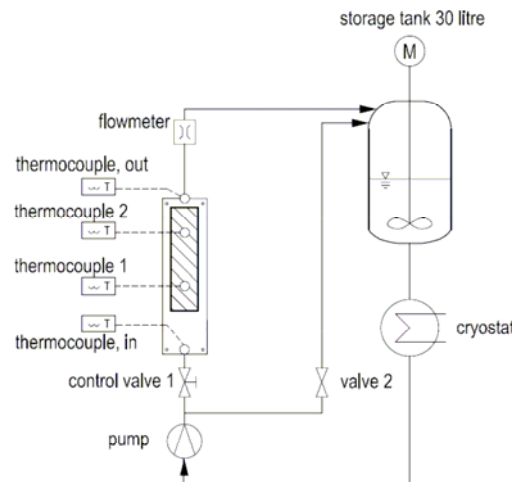

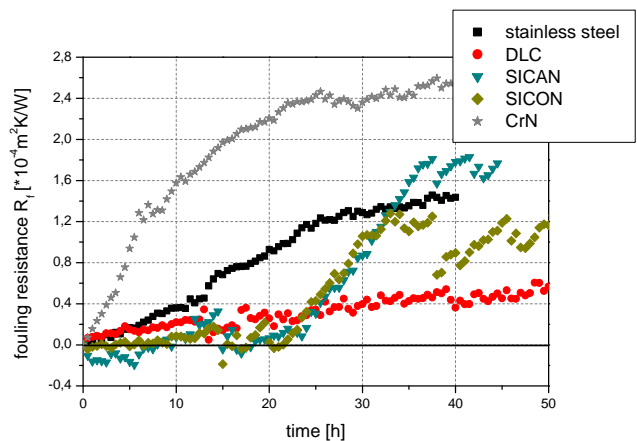Fig. 16: Miniplant unit for fouling experiments with defined flow conditions

Fig. 17: Fouling curves for different coatings on stainless steel (Re = 1,030)

Fig. 17 displays the fouling behavior of coated surfaces in the form of fouling resistance versus time for medium fluid velocity. Chromium nitride shows the highest fouling tendency. The use of coated heat transfer surfaces can increase the induction time for medium fluid velocity compared to stainless steel. By increasing the fluid velocity, the shear stress increases and the slope of the fouling curve should decrease (compare Eq. 1). Low adhesive surfaces like SICON® should benefit from this variation of the process parameter. Fig. 18 shows the fouling curves for the higher fluid velocity (Re 3,100). The induction time

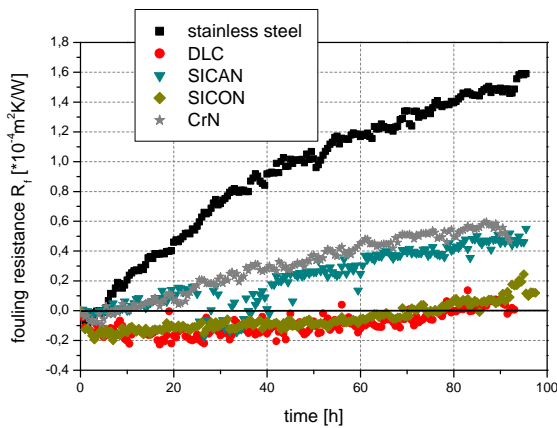compared to uncoated stainless steel can be extended by the factor of 14 (DLC and SICON®).

Fig. 18: Fouling curves for different coatings on stainless steel (Re = 3,100)

The low adhesive interface of DLC coatings (for example SICAN) combined with the decline of first crystallization spots through surface pretreatment can reduce the fouling tendency once more.

Fig. 19 shows the effect of coating on the fouling tendency with higher fluid velocity. The combination of electrochemical treatment and PECVD coating is able to increase the induction time much more than the untreated coated surface. A closer look to economic efficiency of coated heat transfer surfaces should detect, if this additional process step is profitable.
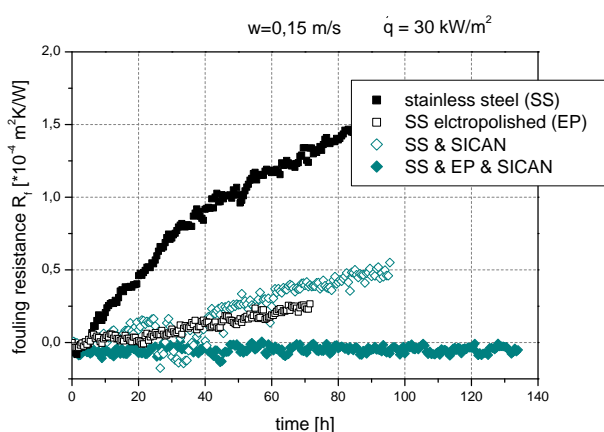

Fig. 19: Fouling curves for SICAN coating on stainless steel (Re = 3,100)

The fouling process should be subdivided into two major influences:

- The crystallization (amount of points and growth) is the key factor for lower fluid velocities.

- By increasing the Reynolds number, the interaction between surface and fouling layer becomes more important. Here, the adhesion is the key factor.

CONCLUSIONS

Fouling experiments with different coated heat transfer surfaces at different fluid velocities have been attempted. The coated surfaces are showing less fouling tendency compared to the uncoated surfaces. The coating of the surface leads to a modified crystallization behavior (micro- and macroscopic). This energetic modification is influencing the first crystallization steps and leads to different growth characteristics of the crystals. The experiments are demonstrating, that with higher fluid velocities the low adhesive characteristics of the coated surfaces lead to longer induction times. By subdividing the major influences on the fouling tendency (crystallization behavior and adhesion), two main strategies for fouling mitigation can be found.

1) Tailored surfaces like SICON® or CrN, which are forcing the crystallization but are low adhesive. This leads to an extention of the induction time due to the faster growing of the crystals out of the boundary layer so they can be worn out by the fluid shear stress

2) Tailored surfaces like DLC which seems to decelerate the crystal growth and therefore leading to longer induction times

Further research should be focused on the scale-up of the miniplant experiences to industrial dimensions. Besides, other fouling relevant systems (biofouling or whey protein fouling) and other heat transfer surfaces (like commercial plate heat exchanger) must be investigated. All experiments on the modification of heat exchanger surfaces aim to coating of flat surfaces. The authors are now able to produce coatings with the PECVD technique inside a tube. Fig. 20 shows first experimental results. The length of the tube is presently limited to 80 cm, but a new coating unit with a length of two meters will be build up. Future research should compare the results of coated plate surfaces with inside coated tubes.
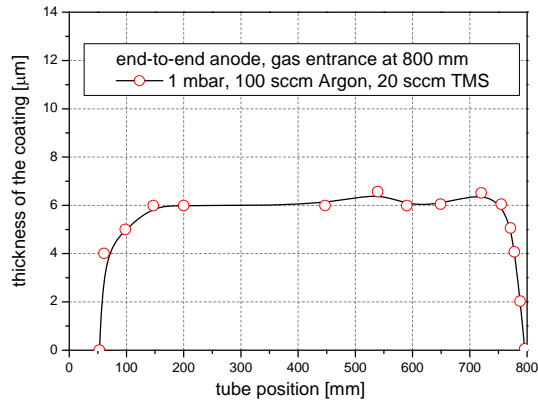
Fig. 20: PECVD coating experiments inside tubes

ACKNOWLEDGEMENT

NOMENCLATURE

A   area, m^2

c   concentration, mol l^{-1}

$\dot{m}$ mass flow, kg s^{-1}

$\dot{Q}$ heat duty, W

R_f fouling resistance, m^2 K W^{-1}

R_Z mean roughness depth, m

t   time, s

w   flow velocity, m s^{-1}

Z   height of the roughness Profile, m

γ_{ij} interfacial free energy between two adjacent phases i and j, N m^{-1}

θ   contact angle, °

Subscript

0   clean

l   liquid

2   solid

3   gas

d   deposition

D   dispersive

f   fouling

fluid   fluid

ind   induction period

P   polar

REFERENCES

[1] Bewilogua, K., Hieke, A., Bialuch, I., Brand, J. and Wittorf, R., "DLC Based Coatings- Preparation, Properties and Applications," *Modern plasma surface technology : 13th International Summer School Mielno 2002,* 2002, pp. 45-52.

[2] Bhushan, B., *"Springer handbook of nanotechnology: with. 71 tables"* Springer, ISBN: 20043-540-01218-4.

[3] Dyckerhoff, G. and Sell, P., *"Über den Einfluss der Grenzflächenspannung auf die Haftfestigkeit"* Die Angewandte Makromolekulare Chemie, no. 21, 1972, pp. 169-185.

[4] Förster, M., Augustin, W., Bohnet, 1999, M., Influence of the Adhesion Force Crystal/Heat Exchanger Surface on Fouling Mitigation, *Chem. Engng. Process.* Vol. 38, pp. 449-461

[5] Förster, M. and Bohnet, M., 2000, Modification of Molecular Interactions at the Interface Crystal/Heat Transfer Surface to Minimize Heat Exchanger Fouling, *Int. J. Th. Sci.*, Vol. 39, pp. 697-708

[6] Trojan, K., Grischke, M. and Dimigen, H., *"Network Modification of DLC Coatings to Adjust a Defined Surface Energy"* Physica status solidi / A. - Berlin : Wiley-VCH, vol. 145, 1994, pp. 575-586.

[7] Zettler, H., Weiß, M., Zhao, Q. and Müller-Steinhagen, H., *"Influence of Surface Properties and Characteristics on Fouling in Plate Heat Exchangers"* Heat Transfer Engineering, no. 26, 2005, pp. 3-17.